SAMSUNG

White Paper

# Utility of S-Shearwave Imaging™ for the prediction of prostate cancer

RS85 Prestige

Prof. Chan Kyo Kim, M.D.

Department of Radiology, Samsung Medical Center,
Sungkyunkwan University School of Medicine

# Introduction

## Background

Prostate cancer (PCa) is clinically suspected based on the results of digital rectal examination (DRE) and/or elevated serum prostate-specific antigen (PSA) level. DRE is subjective and operator dependent, and its sensitivity is questionable for deep or small lesions [1]. It has limited accuracy for staging disease and locating the different foci [2], which are two factors mandatory for planning primary therapy. Despite the low specificity of PSA testing and the low sensitivity of systematic biopsy (SB), these techniques remain the standard of care for PCA diagnosis, mainly because of their widespread availability and low cost [3-6].

The standard for pathologic diagnosis in the men with clinical suspicion of PCa is gray-scale transrectal (TRUS)-guided 10–12 core systematic biopsy. However, this diagnostic pathway using gray-scale TRUS has limited sensitivity (17–57%) and specificity (40–63%) for PCa detection [7]. It is difficult to detect prostate lesions accurately as approximately 58% of PCa cases are multifocal, progress along the prostatic capsule, and may not be seen as well-defined nodules as in other malignant tumors [8]. Furthermore, suspicious hypoechoic areas demonstrate PCa in only 9%–53% of cases [9,10].

PCa has higher cell and vessel density and accordingly, it can be stiffer than benign prostatic tissues [11,12]. Strain elastography has demonstrated the potential for improving PCa detection, with pooled sensitivity and specificity of 67% and 71% [13]. However, this technique has several disadvantages in daily clinical practice, including manual compression, reader dependency, and lack of quantitative data. To overcome these limitations, shear wave elastography (SWE) has been proposed as a noninvasive tool that can provide quantitative stiffness information for tissues in real time. To date, many studies have reported the potential results of SWE in detecting PCa, with various ranges of the sensitivity of 43–96% and specificity of 69–96% [14-18].

Of the several SWE techniques, two-dimensional SWE (2D-SWE) is the tool that uses acoustic radiation force, and several commercially available systems have been developed

[19].

S-Shearwave Imaging™ from Samsung Medison, which generates shear waves using multiple acoustic radiation forces to provide a reliable measurement index (RMI) map, has been developed. The purpose of this white paper is to assess the diagnostic performance of S-Shearwave Imaging™ for predicting PCa.

## Materials and Methods

### Study population

From September 2020 to April 2021, 40 patients with suspected PCa referred to perform MRI-TRUS fusion-guided biopsy from the urology to our department at our institution enrolled in this study. Inclusion criteria were as follows: 1) age $\geq$ 40 years and $\leq$ 80 years; 2) prostate-specific antigen (PSA) level $\geq$ 2.5 ng/ml with or without a target lesion on prebiopsy mpMRI; and 3) performing a 2D-SWE, followed by standard systemic 12-core biopsy with and without targeted biopsy. The exclusion criteria were as follows: 1) age < 40 years or > 80 years, 2) previous radiotherapy or chemotherapy in the pelvis, 3) rectal stenosis due to previous surgery, and 4) denial of participation in this study. Two patients withdrew their consent. Finally, 38 consecutive patients who met the eligibility criteria were enrolled. The mean age was 60.4 years (range, 40–80 years). Institutional review board approval was obtained for this prospective study, and all patients provided written informed consent (IRB No. 2019-08-145).

### TRUS and S-Shearwave Imaging™ examination

Transrectal ultrasound (TRUS) was performed using an ultrasound system (RS85, Samsung Medison, Co., Ltd) equipped with an EA2-11AR transrectal probe by one radiologist with > 10 years' experience in genitourinary US examination. Gray-scale US and 2D-SWE imaging were performed. After volume measurement and routine imaging, the prostate was divided into 12 sectors for both SWE imaging and MRI-TRUS fusion-guided systemic biopsy, with and without a targeted biopsy.

S-Shearwave Imaging™, referred to as 2D-SWE, generates an image that include both

the stiffness and RMI maps. SWE imaging was performed by generating shear wave using a sonographic push pulse, which expresses the tissue stiffness in a color-coded map of Young's modulus (E, kPa), which is simply the ratio of stress placed on a material to the deformation caused by stress, overlaid on gray-scale imaging. According to the World Federation for Ultrasound in Medicine and Biology guidelines [8], SWE was performed in all patients. The field of view of SWE imaging was placed in the right and left lobes in the axial plane. To ensure stable acquisition of the SWE data, the least possible pressure was applied to the prostate while maintaining contact with the probe for 2–4 seconds. For each of the 12 sectors, one circular region of interest (ROI) with diameters of 3–5 mm was placed along the estimated path for the systemic standard biopsy to calculate the Young's modulus (Figure 1).

In addition, regarding target lesions seen on prebiopsy mpMRI, lesion echogenicity on gray-scale US and vascularity on color Doppler US were evaluated, and stiffness on SWE imaging was measured. We also searched for focal lesions on gray-scale US or SWE imaging. To minimize the possible measurement variability on SWE, the stiffness was measured for ROIs with RMI $\geq$ 0.5, and measurements were performed twice, with the corresponding mean value used to represent the stiffness of each ROI. Three quantitative SWE parameters were generated: the maximum Young's modulus of stiffness ($E_{max}$), mean Young's modulus of stiffness ($E_{mean}$), and minimum Young's modulus of stiffness ($E_{min}$).

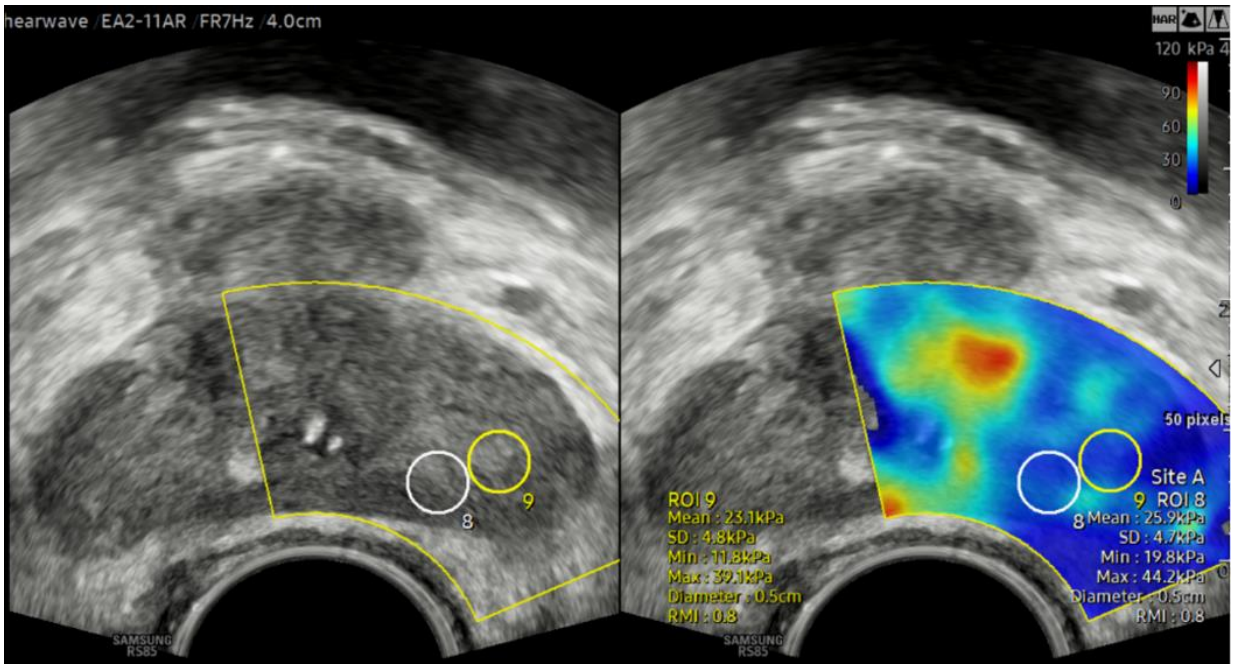


Figure 1. Methods of acquisition for the 2D-SWE parameters. 2D-SWE images in a 58-year-old man show two 5-mm regions of interest on axial gray-scale US (left-sided) and SWE (right-sided) images, placed along the estimated path of the core biopsy in the left peripheral zone of base.

- ## Prebiopsy MRI and MRI-TRUS fusion biopsy

Diagnostic performances including sensitivity, specificity, positive predictive value (PPV), negative predictive value (NPV), accuracy was calculated and compared using generalized estimated equation (GEE) method. Cutoff values for each elasticity value were calculated using the area under the receiver operator characteristics (ROC) curve (AUC) and compared using the Delong's method.

- ## Statistical Analysis

All According to the biopsy results, patients were divided into two groups: patients with PCa and without PCa. The clinical parameters were compared between the two groups.

To predict all PCa and CSC, the diagnostic performance of the clinical or SWE parameters per patient and per region was evaluated using a receiver operating characteristic (ROC) curve analysis. The optimal cut-off values of the parameters were determined using the greatest Youden index. The sensitivity, specificity, and area under the ROC curve (AUC) values were derived as the thresholds. In the patient-based analysis, an index tumor was

defined as a tumor with the highest ISUP grading.

For SWE measurements, interobserver reliability and variability in the right lobe, left lobe, and both lobes were evaluated using the intraclass correlation coefficients (ICCs) and the Bland-Altman plots, respectively. The ICC value was determined to provide a reliability that was poor (0.00–0.20), fair (0.21–0.40), moderate (0.41–0.60), good (0.61–0.80), or excellent (0.81–1.00). A two-sided P-value of $< 0.05$ was considered statistically significant.

Associations between tumor SWE parameters and Gleason scores or PI-RADS scores were determined using Spearman's rank correlation analysis.

## Results

### Baseline characteristics

Patient characteristics are presented in Table 1. The median numbers of target biopsies and combined target and systemic biopsy cores were 2 and 14, respectively.

Table 1. Characteristics of patients with and without PCa

| | All (n = 38) | Cancer Positive (n = 17) | Cancer Negative (n = 21) | *P* value |
|---|---|---|---|---|
| Age (year) | 60.4 ± 8.01 | 61.4 ± 7.0 | 59.7 ± 8.9 | 0.529 |
| PSA (ng/ml) | 24.8 ± 5.4 | 45.4 ± 120.3 | 8.1 ± 10.5 | 0.164 |
| Prostate volume (ml) | 40.5 ± 20.2 | 33.2 ± 12.0 | 46.4 ± 23.6 | 0.043 |
| PSA density (ng/ml$^2$) | 0.58 ± 0.14 | 1.05 ± 2.30 | 0.19 ± 0.19 | 0.143 |
| ISUP grade, median | | 2 (1-5) | | |
| 1 | | 4 | | |
| 2 | | 6 | | |
| 3 | | 4 | | |
| 4 | | 2 | | |
| 5 | | 1 | | |
| # cores of target biopsy | 2 (0-4) | 2 (0-4) | 3 (0-4) | 0.18 |
| # cores of target + systemic biopsy | 14 (12-16) | 14 (12-16) | 15 (12-16) | 0.18 |
| PI-RADS on prebiopsy MRI | | | | 0.005 |
| 2 | 8 | 1 | 7 | |
| 3 | 12 | 3 | 9 | |
| 4 | 13 | 8 | 5 | |
| 5 | 5 | 5 | 0 | |
| Target lesion size (mm) | 11.1 ± 8.8 | 14.3 ± 10.2 | 8.5 ± 6.5 | 0.039 |

Note: Data are presented as mean ± standard deviation or number of patients. The parentheses are range. PSA = prostate-specific antigen, ISUP = International Society of Urological Pathology, Prostate Imaging-Reporting and Data System = PI-RADS, P value: statistical comparison between cancer positive and cancer negative.

### Comparisons of SWE parameters in patient/region-based analysis

The results of the quantitative SWE parameters in patient/region-based analysis are shown in Table 2,3.

In 38 patients, the $E_{max}$, $E_{mean}$, and $E_{min}$ values of the cancer positive patients were

significantly higher than the cancer negative patients (P < 0.001) (Table 2)

Table 2. Results of the patient-based analysis in cancer positive and negative

| | All (n = 38) | Cancer Positive (n = 17) | Cancer Negative (n = 21) | P value |
|---|---|---|---|---|
| $E_{max}$ | 61.0 ± 31.3 | 82.8 ± 35.2 | 43.5 ± 10.0 | < 0.001 |
| $E_{mean}$ | 47.9 ± 29.2 | 69.0 ± 33.1 | 31.0 ± 4.5 | < 0.001 |
| $E_{min}$ | 37.4 ± 23.0 | 52.0 ± 27.8 | 25.5 ± 5.6 | < 0.001 |

Note: Data are presented as mean ± SD. $E_{max}$ = maximum Young's modulus, $E_{mean}$ = mean Young's modulus, $E_{min}$ = minimum Young's modulus, P value: statistical comparison between cancer positive and cancer negative.

Of the 488 regions, 78 (16%) had PCa and the remaining 410 (84%) showed no PCa. The ISUP distributions of the 78 PCa regions were as follows: grade 1 (n = 42), grade 2 (n = 21), grade 3 (n = 10), grade 4 (n = 4), and grade 5 (n = 1). The $E_{max}$, $E_{mean}$, and $E_{min}$ values of the regions with PCa were significantly higher than those of regions without PCa (P < 0.001). Furthermore, all SWE parameters of regions with CSC were significantly higher than those of regions without CSC (all P < 0.01)(Table 3).

Table 3. Results of the region-based analysis in prostate cancer and benign prostate tissue

| | Shear modulus from MRE | | | | | |
|---|---|---|---|---|---|---|
| | All (n = 78) | CSC (n = 36) | Non-CSC (n = 42) | (n = 410) | *P*value* | *P*value** |
| $E_{max}$ | 59.4 ± 30.0 | 71.6 ± 33.2 | 49.0 ± 22.6 | 40.9 ± 17.0 | < 0.001 | 0.001 |
| $E_{mean}$ | 47.1 ± 28.4 | 58.3 ± 34.1 | 37.6 ± 18.0 | 28.8 ± 10.5 | < 0.001 | 0.001 |
| $E_{min}$ | 36.4 ± 25.7 | 45.5 ± 31.8 | 28.5 ± 15.5 | 23.2 ± 12.6 | < 0.001 | 0.003 |

Note: Data are presented as mean ± SD. PCa = prostate cancer, CSC = clinically significant PCa

*Comparison between all PCa and cancer-negative.

**Comparison between CSC and non-CSC.

- ## Diagnostic performance of parameters to predict PCa

Table 4 presents the diagnostic performance of several parameters for predicting all PCa and CSC in the patient-based ROC curve analysis. For predicting all PCa, the $E_{mean}$ showed the highest AUC (0.840), followed by $E_{min}$ (0.832), $E_{max}$ (0.804), and PSA density (0.717). With an optimal cut-off value of 41.3 kPa, the sensitivity and specificity of $E_{mean}$ were 70.6% and 100%, respectively. For predicting CSC, the $E_{max}$ showed the highest AUC (0.865), followed by $E_{mean}$ (0.855), $E_{min}$ (0.828), and PSA density (0.749). With optimal cutoff value of 52.4 kPa,

the sensitivity and specificity of $E_{max}$ were 84.6% and 92.0%, respectively.

Table 4. Diagnostic performance of the parameters in predicting CSC in the patient-based ROC curve analysis

| | All PCa (n = 17) | | | | CSC (n = 13) | | | |
|---|---|---|---|---|---|---|---|---|
| Parameter | Cut-off value (kPa) | Sensitivity (%) | Specificity (%) | AUC | Cut-off value (kPa) | Sensitivity (%) | Specificity (%) | AUC |
| $E_{max}$ | 47.1 | 76.5 | 90.5 | 0.804 | 52.4 | 84.6 | 92.0 | 0.865 |
| $E_{mean}$ | 41.3 | 70.6 | 100 | 0.840 | 42.5 | 76.9 | 96.0 | 0.855 |
| $E_{min}$ | 27.1 | 88.2 | 71.4 | 0.832 | 40 | 61.5 | 96.0 | 0.828 |
| Age | 54 | 94.1 | 28.6 | 0.564 | 61 | 69.2 | 60.0 | 0.610 |
| PSA | 10.9 | 29.4 | 95.2 | 0.560 | 7.51 | 61.5 | 80.0 | 0.680 |
| PSA density | 0.13 | 76.5 | 61.9 | 0.717 | 0.135 | 84.6 | 64.0 | 0.749 |

Table 5 presents the diagnostic performance of the SWE parameters in predicting all PCa and CSC in the region-based ROC curve analysis. Of the 78 regions with PCa, 36 had CSC and the remaining 42 had no CSC. For predicting all PCa and CSC, the AUCs of the $E_{mean}$ were 0.713 and 0.772, respectively, followed by $E_{max}$ and $E_{min}$. With optimal cut-off values of 41.1 and 47 kPa of the $E_{mean}$, the sensitivity and specificity were 43.6% and 87.6% for predicting all PCa, and 50.0% and 92.4% for predicting CSC, respectively

Table 5. Diagnostic performance of the parameters in predicting all PCa and CSC in the region-based ROC curve analysis

| | All PCa (n = 78) | | | | CSC (n = 36) | | | |
|---|---|---|---|---|---|---|---|---|
| Parameter | Cut-off value (kPa) | Sensitivity (%) | Specificity (%) | AUC | Cut-off value (kPa) | Sensitivity (%) | Specificity (%) | AUC |
| $E_{max}$ | 49.8 | 52.6 | 75.7 | 0.684 | 57.3 | 58.3 | 86.1 | 0.772 |
| $E_{mean}$ | 41.1 | 43.6 | 87.6 | 0.713 | 47 | 50 | 92.4 | 0.776 |
| $E_{min}$ | 22.1 | 69.2 | 57.9 | 0.673 | 26.4 | 63.9 | 69.2 | 0.727 |

Note: PCa = prostate cancer, CSC = clinically significant PCa, $E_{max}$ = maximum Young modulus, $E_{mean}$ = mean Young modulus, $E_{min}$ = minimum Young modulus, AUC = area under the curve.

- ## Interobserver reliability and variability

Regarding interobserver reliability, the ICCs of the $E_{max}$, $E_{mean}$, and $E_{min}$ values in the right peripheral zone (PZ) were 0.660 (95% CI, 0.328–0.846), 0.599 (95% CI, 0.236–0.815), and

0.769 (95% CI, 0.512–0.899), respectively; those in left PZ were 0.528 (95% CI, 0.136–0.777), 0.591 (95% CI, 0.225–0.811), and 0.595 (95% CI, 0.229–0.813), respectively; and those in both PZs were 0.542 (95% CI, 0.154–0.785), 0.640 (95% CI, 0.297–0.836), and 0.687 (0.372–0.860), respectively.

For interobserver variability, Bland-Altman plots demonstrated that the mean differences in the $E_{max}$, $E_{mean}$, and $E_{min}$ in the right PZ were 1.5%, 2.7%, and 1.8%, respectively; those in the left PZ were 7.0%, 2.7%, and 0.5%, respectively; and those in both PZs were 5.3%, 0.1%, and 0.6%, respectively.

- ### PCa Associations between SWE parameters and ISUP or PI-RADS

Regarding ISUP grading, the SWE parameters showed significantly poor associations: $E_{max}$ (Spearman coefficient = 0.391, P = 0.004)), $E_{mean}$ (Spearman coefficient = 0.324, P < 0.001), and $E_{min}$ (Spearman coefficient = 0.259, P = 0.022) (all P < 0.001).

The PI-RADS score was moderately correlated with $E_{max}$ (Spearman coefficient = 0.602, P < 0.001), $E_{mean}$ (Spearman coefficient = 0.587, P < 0.001), and $E_{min}$ (Spearman coefficient =0.562, P < 0.001) (all P < 0.001).

## Conclusion

Our results demonstrate that the values of all quantitative parameters derived from the 2D-SWE imaging were significantly higher than those of benign prostate tissues in patient-based and region-based analyses. In the ROC curve analysis, SWE parameters revealed good diagnostic performance for predicting CSC in both patient-based and region-based analyses. Regarding the SWE parameter measurements, the interobserver reliability was moderate to good. These findings indicate that as a reproducible tool, 2D-SWE imaging might offer useful information for differentiating between PCa and benign prostate tissues and for the prediction of CSC. We believe that $E_{max}$ and $E_{min}$ parameters as well as $E_{mean}$ on SWE can be used to evaluate PCa.

The results of our study demonstrate that 2D-SWE imaging is a reproducible tool that provides useful information for differentiating between patients with prostate cancer and

those with benign prostate tissues, as well as predicting clinically significant cancer. Specifically, the quantitative parameters derived from 2D-SWE imaging, including $E_{max}$, $E_{min}$, and $E_{mean}$, were significantly higher in patients with prostate cancer than in those with benign prostate tissues, according to both patient-based and region-based analyses. Additionally, our analysis of the ROC curve showed that these SWE parameters had good diagnostic performance in predicting clinically significant cancer. We also found that the interobserver reliability of SWE parameter measurements was moderate to good, suggesting that 2D-SWE imaging can be a reliable and reproducible method for evaluating prostate cancer. Therefore, we believe that 2D-SWE imaging can be a valuable tool for clinicians in the diagnosis and management of patients with prostate cancer.

In conclusion, the 2D-SWE method appears to be useful for the prediction of PCa. Furthermore, 2D-SWE is a particularly valuable tool for guiding targeted biopsies in urology. It has been observed that lesions can shift in location between MRI and ultrasound-guided biopsy, resulting in a high incidence of specimen errors. This is due to various factors such as the patient's body position and breathing that can affect the lesion's location during the biopsy. In many cases, confirming the lesion on a gray scale US image alone can be challenging, especially for patients with only high PSA levels and no MR results. In such cases, using 2D-SWE as a guide for Target Biopsy is expected to be beneficial. This study is important as it evaluates the performance of 2D-SWE in a patient population with elevated PSA levels that are challenging to determine as either cancer-positive or negative.

## Supported Systems

- RS85 Prestige

## References


1. Smith DS, Catalona WJ. Interexaminer variability of digital rectal examination in detecting prostate cancer. Urology 1995;45:70–74.
2. Baumgart LA, Gerling GJ, Bass EJ. Characterizing the range of simulated prostate abnormalities palpable by digital rectal examination. Cancer Epidemiol 2010;34:79–84.
3. Heidenreich A, Bellmunt J, Bolla M, Joniau S, Mason M, Matveev V, et al. EAU guidelines on prostate cancer: Part I. Screening, diagnosis, and treatment of clinically localised disease. Actas logicas Espanolas 2011;35:501–514.
4. Mottet N, Bellmunt J, Briers E, van den Bergh R, Bolla M, van Casteren N, , et al. Guidelines on prostate cancer. European Association of Urology 2015.
5. Norberg M, Egevad L, Holmberg L, Sparen P, Norlen B, Busch C. The sextant protocol for ultrasound-guided core biopsies of the prostate underestimates the presence of cancer. Urology 1997;50:562–566.
6. Veiga F, Reixa J, Lopez A, Rosado E, Martin M. Current role of PSA and other markers in the diagnosis of prostate cancer. Archivos Espanoles de Urologia 2006;59:1069–1082.
7. Seitz M, Scher B, Scherr M, Tilki D, Schlenker B, Gratzke C, et al. [Imaging procedures to diagnose prostate cancer]. Urologe A 2007;46:W1435-1446; quiz W1447-1438.
8. Barr RG, Cosgrove D, Brock M, Cantisani V, Correas JM, Postema AW, et al. WFUMB Guidelines and Recommendations on the Clinical Use of Ultrasound Elastography: Part 5. Prostate. Ultrasound Med Biol 2017;43:27-48.
9. Beerlage HP, Aarnink RG, Ruijter ET, Witjes JA, Wijkstra H, Van De Kaa CA, et al. Correlation of transrectal ultrasound, computer analysis of transrectal ultrasound and histopathology of radical prostatectomy specimen. Prostate Cancer Prostatic Dis 2001;4:56-62.
10. Junker D, De Zordo T, Quentin M, Ladurner M, Bektic J, Horniger W, et al. Real-time elastography of the prostate. Biomed Res Int 2014;2014:180804.
11. Salomon G, Kollerman J, Thederan I, Chun FK, Budaus L, Schlomm T, et al. Evaluation of prostate cancer detection with ultrasound real-time elastography: a comparison with step section pathological analysis after radical prostatectomy. Eur Urol 2008;54:1354-1362.

12. Konig K, Scheipers U, Pesavento A, Lorenz A, Ermert H, Senge T. Initial experiences with real-time elastography guided biopsies of the prostate. J Urol 2005;174:115-117.

13. Hwang SI, Lee HJ, Lee SE, Hong SK, Byun SS, Choe G. Elastographic Strain Index in the Evaluation of Focal Lesions Detected With Transrectal Sonography of the Prostate Gland. J Ultrasound Med 2016;35:899-904.

14. Ahmad S, Cao R, Varghese T, Bidaut L, Nabi G. Transrectal quantitative shear wave elastography in the detection and characterisation of prostate cancer. Surg Endosc 2013;27:3280-3287.

15. Zhang M, Wang P, Yin B, Fei X, Xu XW, Song YS. [Transrectal shear wave elastography combined with transition zone biopsy for detecting prostate cancer]. Zhonghua Nan Ke Xue 2015;21:610-614.

16. Rouviere O, Melodelima C, Hoang Dinh A, Bratan F, Pagnoux G, Sanzalone T, et al. Stiffness of benign and malignant prostate tissue measured by shear-wave elastography: a preliminary study. Eur Radiol 2017;27:1858-1866.

17. Woo S, Kim SY, Cho JY, Kim SH. Shear wave elastography for detection of prostate cancer: a preliminary study. Korean J Radiol 2014;15:346-355.

18. Boehm K, Salomon G, Beyer B, Schiffmann J, Simonis K, Graefen M, et al. Shear wave elastography for localization of prostate cancer lesions and assessment of elasticity thresholds: implications for targeted biopsies and active surveillance protocols. J Urol 2015;193:794-800.

19. Sigrist RMS, Liau J, Kaffas AE, Chammas MC, Willmann JK. Ultrasound Elastography: Review of Techniques and Clinical Applications. Theranostics 2017;7:1303-1329.

20. Weinreb JC, Barentsz JO, Choyke PL, Cornud F, Haider MA, Macura KJ, et al. PI-RADS Prostate Imaging - Reporting and Data System: 2015, Version 2. Eur Urol 2016;69:16-40.

21. Turkbey B, Rosenkrantz AB, Haider MA, Padhani AR, Villeirs G, Macura KJ, et al. Prostate Imaging Reporting and Data System Version 2.1: 2019 Update of Prostate Imaging Reporting and Data System Version 2. Eur Urol 2019;76:340-351.

22. Srigley JR, Delahunt B, Samaratunga H, Billis A, Cheng L, Clouston D, et al. Controversial issues in Gleason and International Society of Urological Pathology (ISUP) prostate cancer grading: proposed recommendations for international implementation. Pathology 2019;51:463-473.1.

## Disclaimer

* The features mentioned in this document may not be commercially available in all countries.
  Due to regulatory reasons, their future availability cannot be guaranteed.
* Prestige is not a product name but is a marketing terminology.
* Do not distribute this document to customers unless relevant regulatory and legal affairs officers approve such distribution.
* Images may have been cropped to better visualize its pathology.
* This clinical practice review is a result of a personal study conducted by collaboration between Samsung Medison and Prof. Chan Kyo Kim
* This review is to aid customers in their understanding, but the objectivity is not secured..

* 본 자료는 삼성메디슨이 연구자와 협업하여 산출된 연구의 결과물입니다.
  고객의 요청에 따라 이해를 돕기 위해 제공하는 자료일 뿐 객관성은 확보되지 않았습니다.

**For more information, please visit the official website** www.samsunghealthcare.com

**SAMSUNG MEDISON CO., LTD.**


WP202304-S-Shearwave Imaging™